Journal of Micromechanics and Microengineering

Reliability of spring interconnects for high channel-count polyimide electrode arrays

OPEN ACCESS
IOP Publishing
Journal of Micromechanics and Microengineering
J. Micromech. Microeng. **28** (2018) 055007 (9pp)
https://doi.org/10.1088/1361-6439/aaaf2c

Reliability of spring interconnects for high channel-count polyimide electrode arrays

Sharif Khan[1,3], **Juan Sebastian Ordonez**[2] and **Thomas Stieglitz**[1]

[1] Laboratory for Biomedical Microtechnology, IMTEK, University of Freiburg, Freiburg, Germany
[2] Indigo Medical N.V., Gent, Belgium

E-mail: sharif.khan@imtek.uni-freiburg.de

Received 15 December 2017, revised 8 February 2018
Accepted for publication 14 February 2018
Published 8 March 2018

Abstract

Active neural implants with a high channel-count need robust and reliable operational assembly for the targeted environment in order to be classified as viable fully implantable systems. The discrete functionality of the electrode array and the implant electronics is vital for intact assembly. A critical interface exists at the interconnection sites between the electrode array and the implant electronics, especially in hybrid assemblies (e.g. retinal implants) where electrodes and electronics are not on the same substrate. Since the interconnects in such assemblies cannot be hermetically sealed, reliable protection against the physiological environment is essential for delivering high insulation resistance and low defusibility of salt ions, which are limited in complexity by current assembly techniques. This work reports on a combination of spring-type interconnects on a polyimide array with silicone rubber gasket insulation for chronically active implantable systems. The spring design of the interconnects on the backend of the electrode array compensates for the uniform thickness of the sandwiched gasket during bonding in assembly and relieves the propagation of extrinsic stresses to the bulk polyimide substrate. The contact resistance of the microflex-bonded spring interconnects with the underlying metallized ceramic test vehicles and insulation through the gasket between adjacent contacts was investigated against the MIL883 standard. The contact and insulation resistances remained stable in the exhausting environmental conditions.

Keywords: gasket underfill, spring interconnects on flexible electrode arrays, implantable systems

(Some figures may appear in colour only in the online journal)

Introduction

Advances in neuroscience have been accelerating the number of simultaneously recorded cells in the brain. It has been predicted that the number of simultaneous neurons recordings doubles every 7 years, projecting the ability to record 1000 neurons in the next 10 years [1]. Though the progress in neuronal data analysis techniques and high speed processing are important factors, the transition from a single wire electrode to multiple electrode arrays has played a vital role in this development. However, an associated challenge with increasing the channel-counts is the assembly of the recording or stimulation arrays with amplifiers and electronics for wireless data transmission.

A fully implantable system for brain-machine interfacing should be capable of wireless transcutaneous communication for clinical viability [2]. The power modules, data acquisition or sense/stimulation circuitry and telemetry units along with the antenna(s) should be an integral part of the compact implant system. Though the implant electronics are sealed on the component or system level [3–5], their interconnections interface with the electrode arrays is usually prone to attack from the physiological environment. This issue is not very critical for implants with stiff electrode substrates

[3] Author to whom any correspondence should be addressed.

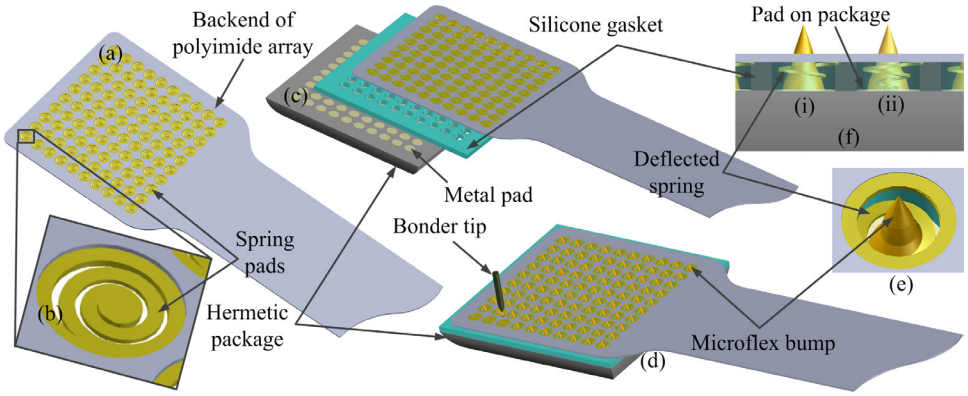

Figure 1. Conceptual illustration of implant assembly with spring interconnects on polyimide array (not to scale); (a) backend of electrode array with 10 × 10 interconnects array; (b) close-up view of a single spring interconnect; (c) exploded view of assembly sequence with silicone gasket isolation; (d) microflex bonding of polyimide array on metallized package; (e) close-up view of a single microflex bonded spring pad; (f) conceptual illustration of spring pad deflected under microflex bond shown in (i) downward procession of spring with microflex through transparent underfill gasket (ii) conceptual view of the microflex anchoring the circular seating of the spring with the rigid substrate (microflex shown transparent for illustration).

(such as silicon) since the electronics can be monolithically integrated or can be bonded and sealed on the silicon substrate reliably because of well-established technology [6, 7]. However, the problem still persists in implants with flexible electrode arrays. Even if the electronic package is hermetic, it is impossible to seal the interconnections interface hermetically with existing technologies. Their protection against the environment can only be ensured by sophisticated underfilling and encapsulation with ion-blocking adhesive materials [8–12]. The risks to the reliability of such hybrid assemblies are enhanced for implants with a high channel-count such as retinal implants [5, 13]. The limited physiological space (for implant) leads to a high density of interconnects, which deters perfect underfilling with widely used capillary flow adhesives in implants. In previous work, authors have suggested a pre-structured polydimethylsiloxane (PDMS) silicone sheet as the solid-underfill for high-density interconnect applications [14]. Additionally, a bottom-to-top thin-film fabrication process was developed for dual-sided graded interfaces on a polyimide array for improved adhesion with the gasket as well as the glob-top encapsulation [15, 16].

The careful selection of surface finishing on mating interfaces combined with a silicone gasket underfill will provide long-term reliability of interconnects as well as assembly. Adversely, the gasket introduces a permanent gap between the backend of the flexible array and the rigid substrate. Consequently, the electrical bonding will induce warpage and excessive extrinsic stresses in the thin film layers as well as their interface with the gasket. This will increase the likelihood of delamination at the gasket interface and will make the thin film layers susceptible to buckling in long term applications. A variety of bonding techniques are used for hybrid assemblies [17–24], in which the reliability of bonding might resiliently depend on the nature, process parameters and applied technology.

In this work, spring-type interconnects are fabricated on a polyimide array and characterized together with a silicone gasket insulation. The microflex technique is used to establish electrical contact between the polyimide array and rigid substrate. Mechanically flexible interconnects with a fixed vertical height are widely investigated for flip-chip assembly on rigid substrates [25–30]. These interconnects minimize the thermo-mechanical stresses due to the mismatch in coefficients of thermal expansion and compensate for the non-planer surface of the substrate as well as potentially allowing rematable connections. Spring interconnects on flexible arrays is a novel concept. In contrast to the compliant contacts on the rigid substrate, the helically shaped interconnects on the polyimide are fabricated in-plane with the substrate and extend towards the pads on the package upon bonding. The conceptual schematic of the assembly illustration of a polyimide array with spring interconnects is shown in figure 1. The spring properties of the interconnects overcome the physical gap disposed by the gasket underfill between the flexible array and electronics package. Each helical spring features a circular end at the center, which provides a seating pad for the microflex bond. The bonder tip deflects the spring downward releasing the microflex bump, which anchors the circular seating to the metal pad on the rigid substrate (figures 1(d)–(f)). Additionally, it minimizes the transformation of the bonding induced stresses from the interconnect pads to the bulk polyimide substrate thereby reducing the risk of delamination of the thin film layers and their loss of adhesion with the gasket underfill. Therefore, the combination of the spring interconnects on the flexible electrode arrays with the silicone gasket underfills in the implant assembly is expected to improve the reliability of fully implantable systems.

Materials and methods

The test assembly for compliant interconnects consists of a polyimide-based platinum interconnects array, a ceramic package and a silicone gasket as the underfill insulation. The fabrication of these assembly elements and the integration process is described below.

Fabrication of spring interconnects

A 10 × 10 matrix array of spring interconnects in a helical design over a total area of 4.8 × 4.8 mm was fabricated on a

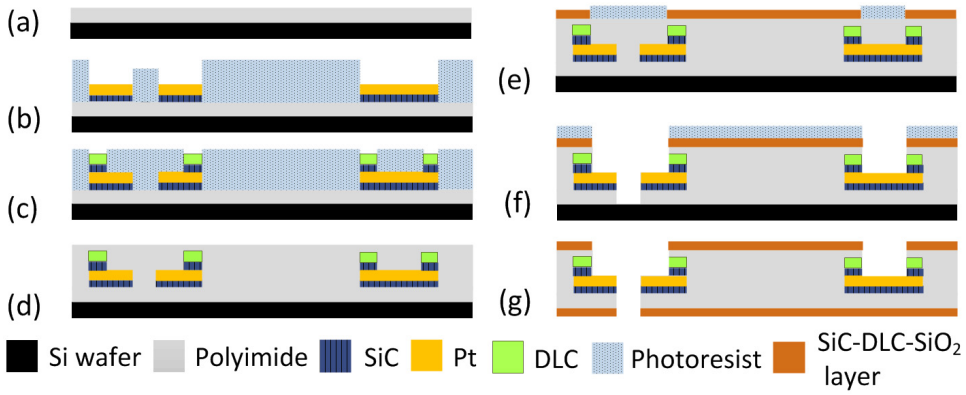

Figure 2. Fabrication process steps for polyimide microelectrode array with spring interconnect. (a) Spin coating of polyimide film; (b) deposition of SiC and Pt; (c) deposition of SiC and DLC adhesion layers; (d) spin coating of top polyimide insulation; (e) PECVD of graded layers SiC, DLC and SiO_2 in sequence; (f) polyimide etching of contact and electrode sites and contours; (g) detachment and deposition of graded layers on the bottom side.

polyimide substrate replicating the backend of an electrode array. Each 20 μm wide helix (with arc length of 240 μm) extended from a circular annulus with a 150 μm inner diameter and 490 μm center-to-center pitch. The fabrication started with spin coating the polyimide (U-varnish-S) resin on the 4 inch silicon wafer and curing in nitrogen at 400 °C for 3 h, resulting in a final thickness of 5 μm (figure 2(a)). Next, a 1.4 μm thick layer of image reversal photoresist was spin coated and lithographically patterned as the metallization mask. A 50 nm thin layer of silicon carbide (SiC) was deposited using plasma enhanced chemical vapor deposition (PECVD) as the adhesion promoter between the polyimide and the 300 nm thin evaporated platinum (Pt) layer [31] (figure 2(b)). A second lithography step was carried out for the deposition of 40 nm SiC followed by a 10 nm diamond-like-carbon (DLC) layer as the transitional adhesion promoters between the metal and the top 5 μm thick polyimide layer (figures 2(c) and (d)). Another lithography step was performed for PECVD of the top side graded interface layers of DLC, SiC and SiO_2 (figure 2(e)). The final lithography step was performed to expose the metal interconnect, test pads and structural boundaries using reactive ion etching at room temperature (figure 2(f)). The samples were detached from the carrier wafer and flipped onto a substrate. The graded adhesion promoter layers of DLC, SiC and SiO_2 were then deposited on the bottom side of the structures (figure 2(g)).

Ceramic test vehicles

The test vehicle for investigating the reliability of the compliant interconnects on the electrode arrays and hermetically sealed electronics were fabricated by metallizing an alumina (Al_2O_3) ceramic with a 10 μm screen printed gold layer 8844-G (ESL, King of Prussia, Pennsylvania, USA). The metallized ceramic was then screen printed with a dual purposed dielectric overglaze layer (ESL 4031-B) covering and insulating the metal tracks while additionally serving as an adhesion layer for the silicone [32].

Gasket underfill

Silicone gaskets have been previously reported on as a solid underfill for active implants with a polyimide substrate [14]. The fabrication process for the gasket is summarized in this section. The PDMS precursor (MED-1000, NuSil, Carpinteria, CA, USA) mixed and centrifuge-spun with an equal volume of n-heptane was spin coated at 5000 rpm for 30 s on an alumina ceramic carrier, which was pre-laminated with adhesive tape (No 4124, Tesa AG, Hamburg, Germany). An approximately 20 μm thick silicone sheet was achieved after evaporation of the solvents. The gasket was manufactured by laser structuring the silicone sheet with a high power passively mode-locked Nd:YVO_4 picosecond laser Rapid 10 (by Lumera Laser, Kaiserslautern, Germany) for conformal structure. A low power and frequency were used in order to avoid excessive burning. The cleaning and release of the gasket from the lamination tape was assisted by cleaning agents such as ethanol.

Assembly

The assembly process of the flexible array with a solid underfill and rigid package follows the schematic illustration depicted in figure 1. The integration began with the assembly of the silicone gasket on the ceramic test vehicle followed by a polyimide interconnections array; prior cleaning and activation of the mating surfaces with cleaning agents and O_2 plasma (performed at 80 W in a low-pressure plasma reactor, Diener Electronic, Germany) was required at each assembly step. The oxygen plasma activates the surface of the silicone rubber sheet and improves its bonding capability [33]. Carrying out the assembly process under the microscope ensured precise positioning and alignment of the mating elements. Additionally, the integration sequence allowed for thorough cleaning of the mating surfaces at every step and assured void- and contamination-free mechanical bonding of the underfill between the rigid device and flexible electrode array prior to electrical bonding. The strong adhesion of the silicone gasket with the overglazed ceramic and polyimide array with a SiO_2 termination layer served as the mechanical bond in the assembly. The electrical

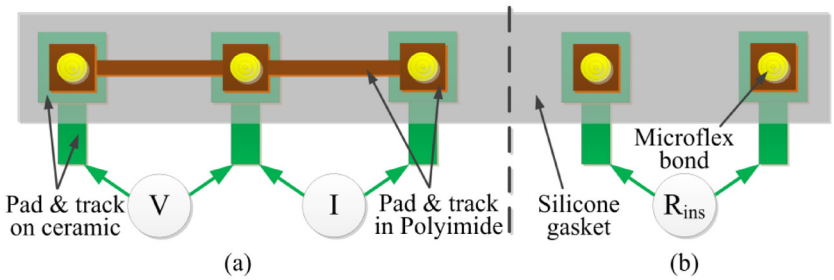

Figure 3. Schematic illustration of (a) contact resistance measurement with four-point probe method on ceramic test vehicle and polyimide substrate. (b) Measurement of pad-to-pad insulation resistance (R_{ins}) through silicone gasket.

contacts were achieved by microflex bonding (using K&S 4524 A, Kulicke & Soffa Industries Inc., Singapore) [21, 22] the compliant interconnects with the corresponding metal pads on the ceramic test vehicle. Finally, the samples were encapsulated with PDMS using a custom mold. Assembly samples without a gasket and encapsulation were also fabricated for reliability tests of the spring interconnects design under dry conditions (with vibration, thermal cycling and high temperature tests). The polyimide arrays were microflex bonded directly onto the metallized ceramic carrier.

Reliability testing of spring interconnects

Test assemblies were used to investigate the performance of the spring interconnects and gasket insulation. The spring interconnects were evaluated in terms of the contact resistance between the spring pad on the polyimide array and the corresponding pad on the ceramic test vehicle through the microflex bond. The resistance was measured using a four-probe method illustrated in figure 3. The sense and input probes were both placed on the ceramic test pads, which led to the pads on the ceramic test vehicle, which in turn were bonded to the under-test spring pads. The conductive paths between the pads were provided through the spring interconnects by the metal tracks in the polyimide substrate. The insulation resistance through the gasket was measured between adjacent interconnections without a conductive link using the four-probe as well as electrochemical methods. The samples were subjected to the following test conditions:

Temperature cycles

The assemblies without a gasket were subjected to 100 thermal cycles (between −40 °C to +140 °C) with a 10 min dwelling time at each temperature as per MIL STD 883 using a climate test chamber VCL 4010 (Weiss Technik, UK). The samples were cooled down to room temperature and taken out of the chamber after the 140 °C phase of intermittently selected cycles. The contact resistance of the spring pads were measured using a 4-point measurement station EP4 (SÜSS Microtech SE, Garching, Germany) with a 34401A multimeter (Hewlett-Packard Company, CO, USA). The samples were also visually inspected under the microscope for any possible fatigue. Test samples were stored again in the chamber after each measurement.

Vibration tests

The mechanical stability of the spring interconnects microflex bonded onto the ceramic test vehicles was investigated using a Tira S 513 vibration shaker with a BAA 120 amplifier (Tira GmbH, Schalkau, Germany). A customized hard fixture was used to hold the samples on the shaker. A vibration was performed at 20 m s^{-2} with a back-and-forth frequency sweep between 20–2000 Hz for 144 h. The resistances of the microflex-bonded springs were measured using the 4-probe setup every 24 h until 100 h and then again at the end of testing.

High temperature storage at 300 °C

The effect of high thermal stresses on the performance of the spring interconnects was also investigated. The microflex bonded samples of the spring interconnect arrays on the ceramic carriers were stored at 300 °C under a continuous dry-nitrogen flow (27 l h^{-1}) for 300 h in a Carbolite furnace (model: CTF 12/65/550, Carbolite Gero Ltd. Sheffield, England). The samples were taken out at regular intervals of 24 h to test the contact resistance with the 4-probe method at room temperature.

Accelerated-age tests in phosphate buffered saline (PBS) solution at 60 °C

The effect of soaked-age testing and volumetric swelling of the silicone gasket due to moisture uptake on the spring interconnects in assembly was investigated. The assembled samples were stored in PBS at 60 °C for accelerated aging in a Heraeus function-line incubator (Thermo Fisher Scientific Inc., MA, USA) such that the encapsulated interconnections assembly on the sample always remained immersed in PBS. The test pads on the ceramic vehicle were exposed through the sealed openings in the lid of the container for measurement purposes. The assembly samples were intermittently taken out of the incubator and the continuity of the interconnections was tested.

The insulation resistance of the gasket between the adjacent interconnects was measured using the same setup used for contact resistance measurement. In addition, the insulation resistance was also investigated using the Solartron SI-1287 Electrochemical Interface with the SI-1260 Impedance/Gain-Phase Analyzer (AMETEK GmbH, Meerbusch, Germany). A sinusoidal voltage of 100 mV was applied between the adjacent interconnects with a frequency sweep of 1–10^5 Hz.

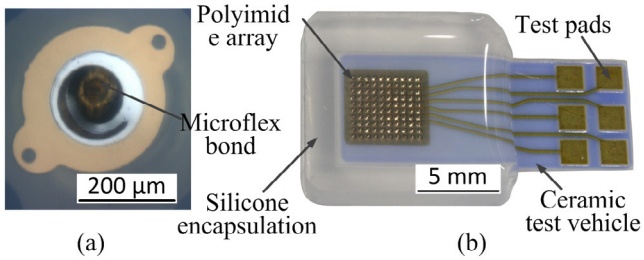

Figure 4. (a) Micrograph of a spring interconnect bonded on ceramic test vehicle using microflex; (b) a PDMS encapsulated sample with silicone gasket sandwiched between polyimide array and ceramic test vehicle.

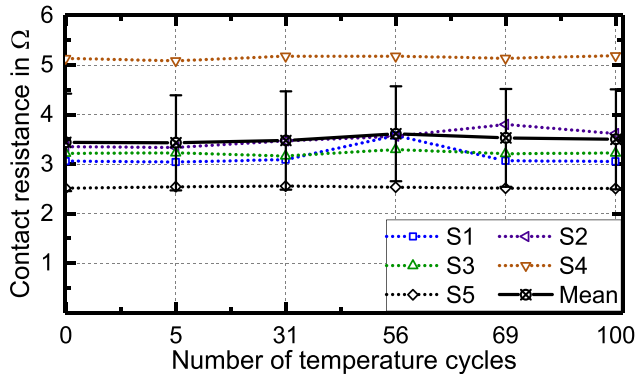

Figure 5. Thermal cycles test, contact resistance for five representative samples (S1–S5) with mean ± Std. during 100 temperature cycles (−40 °C to 140 °C).

Stresses under electric pulses

The assembled samples were also subjected to electrically induced stresses in the PBS solution for the conductivity of flexible interconnects and gasket insulation. A current with alternating negative and positive square pulses each with an amplitude of 1 mA and a duration of 300 μs was applied between the adjacent interconnects. A 20 μs delay was introduced between the alternating flanks. A Plexon stimulator (Plexon Inc, Dallas, Texas, USA) and PicoScope 2206B (Pico Technology, St Neots, Cambridgeshire, UK) were used to simultaneously apply and monitor the applied current as well as the measured voltage. A set of five samples each with three distinct interconnects with a conductive link between the interconnects inside the polyimide insulation was used to measure the contact resistance.

Results

An example of a spring interconnect on the polyimide that was microflex-bonded with the underlying gold pad on the ceramic substrate is shown in figure 4(a). The complete assembly with the silicone encapsulation for the soaked tests in PBS is also shown in figure 4(b). The contact resistance was measured between the ceramic test pads which were connected with the under-test spring pads through screen printed tracks. The measured resistance comprised of the resistance of the gold tracks on the ceramic, the resistance of the microflex bonds and compliant interconnects and the resistance of the short metal track sandwiched in the polyimide. The inter-contact insulation and their environmental isolation was achieved by an ion-blocking silicone gasket.

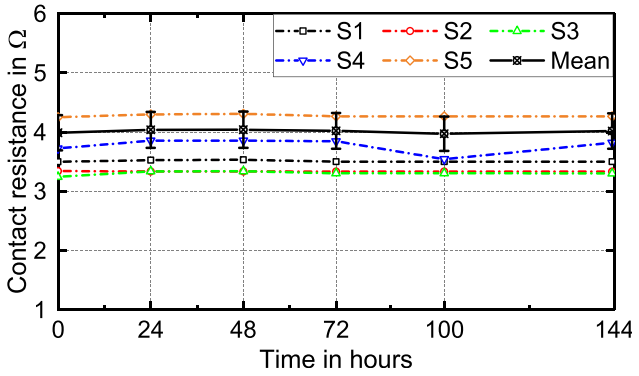

Figure 6. Contact resistance of five representative samples (S1–S5) with mean ± Std. during vibration test.

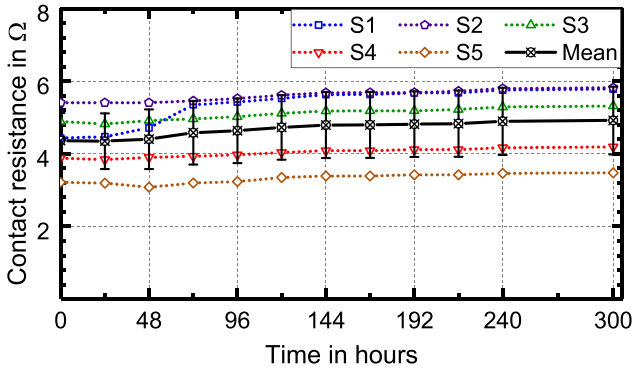

Figure 7. Contact resistance mean ± Std. of five representative samples (S1–S5) during high temperature storage (300 °C) in dry nitrogen.

Temperature cycles

A coherent response in contact resistance of the microflex bonded spring interconnects was observed (figure 5). The measurements were taken initially before starting the tests and after five cycles and then continued at intermittent intervals. A small increase was observed from 3.455–3.512 Ω (with standard deviation (Std.) of 0.9 in both cases) after 100 thermal cycles (approximately 197 h). However, no failure was observed in the spring structures or the microflex bond during the testing period.

Vibration test

The spring interconnects showed a stable response during mechanical reliability testing (figure 6). A minor rise in the average resistance (for $n = 5$) from 3.61 ± 0.36 Ω to 3.64 ± 0.36 Ω after 144 h of vibration testing was found. The visual and microscopic inspection of the samples confirmed the intactness of the spring structures and microflex bonds.

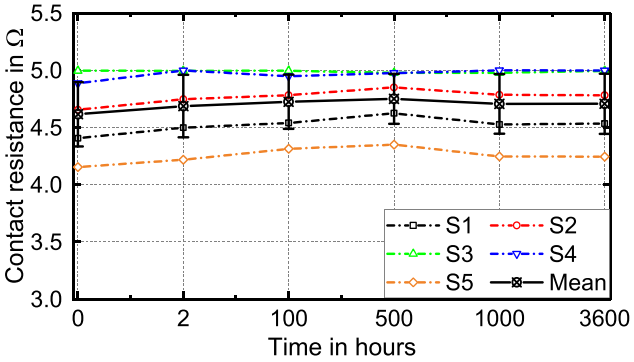

Figure 8. Contact resistance during accelerated aging in PBS at 60 °C for five representative samples (S1–S5) with mean ± Std.

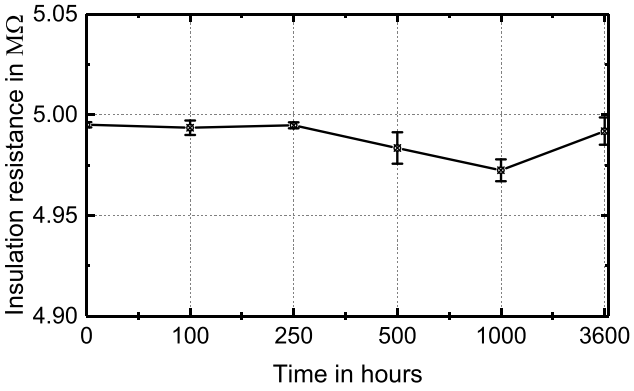

Figure 9. Mean insulation resistance ± Std. of the gasket between adjacent interconnects during accelerated age tests in PBS at 60 °C for 10 samples.

High temperature storage test

The contact resistance of the spring interconnects increased from 4.36 ± 0.76 Ω to 4.91 ± 0.93 Ω during 300 h of high temperature storage at 300 °C in high temperature storage tests (figure 7). However, no failure of the spring contacts was observed in the samples.

Soak tests results

A set of 13 samples was stored in PBS at 60 °C. One of the samples showed a large increase in the contact resistance (from 4.11–9.72 Ω) during the final measurement while the rest of the samples sustained a common trend during the course of the experiment. The tendencies in the contact resistance during 3600 h of testing for five representative samples is shown in figure 8. The resistance increased from 4.63 ± 0.28 Ω to 4.70 ± 0.27 Ω during the first 2 h of storage; a minor rise in resistance was observed (to a final value of 4.72 ± 0.27 Ω) after 3600 h.

The insulation resistance during age testing at 60 °C in PBS was investigated for a set of 11 samples. The 4-point measurements showed a drop in the insulation resistance at a very slow rate from 4.995 ± 0.001 MΩ to 4.991 ± 0.007 MΩ during 3600 h of storage (figure 9). Furthermore, the electrochemical

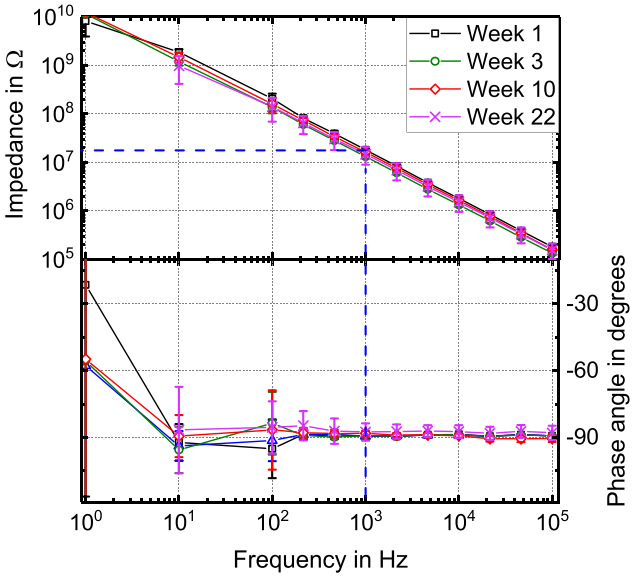

Figure 10. Mean insulation impedance and phase angle of gasket between adjacent interconnects of 10 samples during 22 weeks of accelerated age testing in PBS at 60 °C.

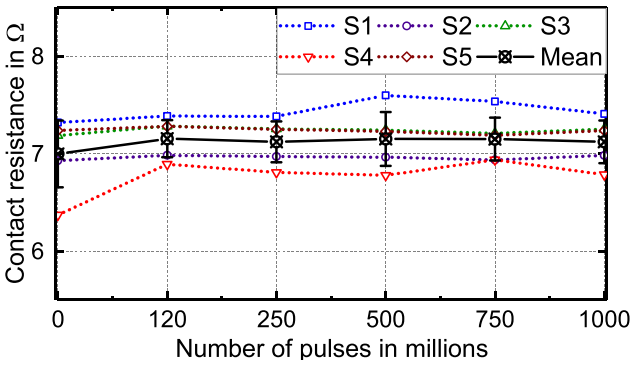

Figure 11. Contact resistance of spring interconnects of five samples (S1–S5) with mean ± Std. subjected to 1 billion current pulses of ± 1 mA and 300 μs duration.

measurements also showed a strong insulation impedance with a very high leakage resistance over a frequency range of 1–10^5 Hz. A set of 10 samples, each with two measurements between a different set of adjacent interconnects (total of 20 measurements per test event) was investigated. The average impedance magnitudes at 1 kHz were 18.00 ± 1.67 MΩ (phase angle of −89°) and 14.71 ± 5.81 MΩ (phase angle of −88°) for the measurements before and after 22 weeks of storage, respectively (figure 10).

Pulse testing

A slight increase in the average contact resistance of the sample set ($n = 5$) from 7.01 ± 0.34 Ω to 7.13 ± 0.22 Ω was observed after exposing the sample to 1 billion pulses (figure 11). A major part of this drift in resistance appeared after 120 million pulses (i.e. 7.16 ± 0.19 Ω), which was almost sustained during the rest of the testing period.

Table 1. Comparison of resistance measurements before and after the tests.

Test conditions		Resistance before	Standard deviation	Resistance after	Standard deviation
Thermal cycles test (100 cycles)		3.455 Ω	0.9 Ω	3.512 Ω	0.9 Ω
Vibration test (144 h)		3.61 Ω	0.36 Ω	3.64 Ω	0.36 Ω
High temperature test (300 h)		4.36 Ω	0.76 Ω	4.91 Ω	0.93 Ω
Accelerated age test (3600 h)	Contact resistance	4.63 Ω	0.28 Ω	4.70 Ω	0.27 Ω
	Insulation resistance	4.995 MΩ	0.001 MΩ	4.991 MΩ	0.00 MΩ
	1 kHz insulation resistance	18.00 MΩ	1.67 MΩ	14.71 MΩ	5.81 MΩ
Pulse test (1 billion pulses)		7.01 Ω	0.34 Ω	7.13 Ω	0.22 Ω

Discussion

A new approach is introduced for the sophisticated assembly of active medical implants involving high density contacts between a flexible electrode array and hermetically sealed electronics. Two critical requirements i.e. the sustainability of interconnections against the environmental stresses and their isolation from each other as well as against an aqueous body environment are addressed. The introduction of the laser structured silicone gasket as the underfill between the flexible array and the electronics package allowed for a pre-bonding underfilling process. Consequently, proper cleaning of the mating surfaces at each assembly step was conceivable, which would otherwise be unlikely; it also allowed for cleaning post-bonding process residues. Therefore, use of a gasket underfill allowed a contamination-free mechanical interface between the assembly elements and eliminated the risk of leakage current due to entrapped ionic contamination when placed in a moist environment [14]. Additionally, the centrifuge spinning of the PDMS resin to evacuate the entrapped air before spin coating ensured a voids-free underfill thereby disallowing room for moisture condensation in assembly. PDMS silicone was chosen for its well-established biocompatibility, stability and wide range application as a substrate and encapsulation material [12, 34, 35]. Another major advantage of a PDMS gasket is its ability to be activated with oxygen plasma for achieving adhesion with the mating surfaces.

The second critical requirement regarding the sustained electrical connections was accomplished by using a spring design for the contact pads on the flexible electrode array. The spring design not only dampened down the stresses introduced in the assembly during integration and bonding process but most importantly, also compensated for the height of the gasket, which created a permanent gap between the flexible array and rigid package. The compliant design of the interconnects also minimized the effects of swelling in the silicone gasket due to its permeability to moisture and water uptake. Due to the damping effect the bonding induced deformations at the bonding pads also minimally affected the rest of the polyimide substrate. Consequently, the risk of delamination of layers with different mechanical properties was reduced. This additionally prevented positional mismatch between the pads on the polymer array and ceramic substrate during bonding because of stresses and resulting buckling/warpage introduced in the polyimide substrate after bonding with some pads, more likely in the high-density interconnect assembly. The spring constant of the multi-layer (and multi-material) spring design was approximated by a tapered helical spring of rectangular wire. The calculations resulted in a total value of 6.34 mN mm^{-1}.

A dual step investigation was carried out; the spring interconnects were tested against intensive vibration, thermal cycles and high temperature against the MIL 883 standard. Secondly, the dummy assemblies with the gasket underfill were tested against the aqueous environment during accelerated age-testing at 60 °C and electric current pulses in PBS. Table 1 presents the summary of electrical measurements against the test conditions. No major change in the resistance of the interconnects was observed during the vibration and temperature cycles test, however, a slight increase in the resistance was observed during high temperature tests 4.36 ± 0.76 Ω to 4.91 ± 0.93 Ω. A similar behavior has been reported previously for MEMS microflex for chip-scale bonding [23]. However, no failure in the tested interconnects was observed due to 'Kirkendall's' effect or 'Horsting' voids [21, 23]. A possible reason could be that the gold metallization on the rigid substrate was screen printed and cured at 950 °C.

The experimental results of the soaked tests (the accelerated aging and pulse testing) have shown that the implant assembly with the gasket underfill and compliant interconnects on the flexible electrode array is reliable against environmental effects. A small increase in the contact resistance was observed. However, a significant part of the change appeared during the initial measurements after exposing the samples to test conditions, which were almost sustained afterwards. It can be deduced from the results that the change in resistance was prominent during the initial hours of soaking when the PDMS was reaching the moisture-uptake saturation. The other parameters (i.e. temperature and electric pulses) then did not have a substantial effect on the contact resistance of the spring interconnects during subsequent test periods. An important aspect of the spring interconnects was to reduce the stresses in the film layers as well as at the interface with gasket. This is essential for sustained adhesion at the interface in order to achieve reliable insulation in long-term applications. The PDMS silicone is a good insulator to ions however it is permeable to moisture. Soaking of the samples results in the absorption of moisture in the silicone gasket [36]. The presence of any voids and process residue contamination would result in the electrochemical migration of ions due to the accumulation and condensation of moisture in the voids and in the vicinity of contamination. This would result in an increased leakage current or a short circuit of interconnects, eventually

leading to the failure of the device. This was observed in two samples with fabricated defects in the glob-top encapsulation, which failed a few hours after storing in PBS. The rest of the samples retained considerably high insulation resistances between the interconnects for both the direct current and electrochemical measurements. A very small drop in the insulation resistance (from 4.995–4.991 MΩ) was observed with 4-point measurements after 3600 h, which corresponds to approximately 24 months in a physiological environment. The high impedance at 1 kHz with highly capacitive behavior also presented a very low leakage current over the testing period. The apparent tendency in drop predicts a stable insulation resistance over a long time, which is considerably higher than the 250 KΩ of the commercially available SYGNUS® implantable contact system [37]. The consistent insulation resistance of the survived samples shows that the silicone gasket underfill, if applied carefully along with globe top silicone encapsulation will increase the life time of the insulation in a physiological environment. It can also be established that the application of spring interconnects successfully avoided excessive extrinsic stresses at the polyimide array and silicone gasket interface. This helped with the intact adhesion at the interface in the presence of environmental stresses.

Conclusion

The age tests in PBS at high temperatures might have additional impacts/hazards compared to actual body environments and some supplementary reactions might happen, which will not actually occur in the body. The gasket sustained high insulation between adjacent interconnects with a final impedance of 14.71 MΩ (and phase angle of −88°) measured at 1 kHz after completion of the accelerated-age testing, which corresponded to ~24 months at 37 °C. The persistent insulation properties of the gasket during accelerated-age conditions makes it a better potential alternative for existing techniques, especially considering the long-term applications. The test results suggest that the spring behavior of the interconnects successfully resisted the transformation of extrinsic stresses to the bulk polyimide while maintaining self-intactness. Furthermore, the spring interconnection pads combined with microflex bonding also maintained their continuity under MIL 883 conformal test conditions, which also largely surpassed the physiological environment. Very minor variations in the average contact resistance of spring interconnects were observed (i.e. from 3.455–3.512 Ω after 100 thermal cycles of −40 °C to +140 °C, 3.61 ± 0.36 Ω to 3.64 ± 0.36 Ω over 144 h of vibration and 4.36 ± 0.76 Ω to 4.91 ± 0.93 Ω after 300 h of storage at 300 °C). The contacts remained stable during accelerated aging with 4.70 ± 0.28 Ω and 4.72 ± 0.27 Ω resistance, respectively, measured after 2 and 3600 h storage in PBS solution at 60 °C. It can be safely concluded that a combination of spring interconnects and gasket underfill would improve the reliability of a long-term fully implantable system with high channel-count and high density interconnections. Furthermore, the spring interconnects on a flexible substrate can also be investigated for potential applications as rematable interconnections in high channel-count arrays.

Acknowledgments

This work was partly supported by the BrinLinks-BrainTools Cluster of Excellence under DFG grant no. EXC 1086. The authors are grateful to Professor Dr Leonhard Reindl, Professor Dr Thomas Hanemann and Mr Taimur Aftab of IMTEK for providing access to their test equipment.

ORCID iDs

Sharif Khan https://orcid.org/0000-0002-7250-7359
Thomas Stieglitz https://orcid.org/0000-0002-7349-4254

References

[1] Stevenson I H and Kording K P 2011 How advances in neural recording affect data analysis *Nat. Neurosci.* **14** 139–42
[2] Lebedev M A and Nicolelis M A 2006 Brain–machine interfaces: past, present and future *Trends Neurosci.* **29** 536–46
[3] Stieglitz T 2010 Manufacturing, assembling and packaging of miniaturized neural implants *Microsyst. Technol.* **16** 723–34
[4] Ordonez J, Dautel P, Schuettler M and Stieglitz T 2012 Hermetic glass soldered micro-packages for a vision prosthesis *Proc. IEEE Engineering in Medicine and Biology Society* pp 2784–7
[5] Guenther T, Lovell N H and Suaning G J 2012 Bionic vision: system architectures: a review *Exp. Rev. Med. Devices* **9** 33–48
[6] Kim S *et al* 2009 Integrated wireless neural interface based on the Utah electrode array *Biomed. Microdevices* **11** 453–66
[7] Wise K D, Anderson D J, Hetke J F, Kipke D R and Najafi K 2004 Wireless implantable microsystems: high-density electronic interfaces to the nervous system *Proc. IEEE* **92** 76–97
[8] Donaldson P E K 1987 The role of platinum metals in neurological prostheses *Platinum Met. Rev.* **31** 2–7
[9] Donaldson P E K and Aylett B J 1995 Aspects of silicone rubber as encapsulant for neurological prostheses *Med. Biol. Eng. Comput.* **33** 285–92
[10] Sutanto J *et al* 2012 Packaging and non-hermetic encapsulation technology for flip chip on implantable MEMS devices *J. Microelectromech. Syst.* **21** 882–96
[11] Donaldson K P E 1987 Twenty years of neurological prosthesis-making *J. Biomed. Eng.* **9** 291–8
[12] Jackson N, Anand S, Okandan M and Muthuswamy J 2009 Nonhermetic encapsulation materials for MEMS-based movable microelectrodes for long-term implantation in the brain *J. Microelectromech. Syst.* **18** 1234–45
[13] Ordonez J S, Schuettler M, Ortmanns M and Stieglitz T 2012 A 232-channel retinal vision prosthesis with a miniaturized hermetic package *Proc. IEEE Engineering in Medicine and Biology Society* pp 2796–9
[14] Khan S, Ordonez J S and Stieglitz T 2016 Laser patterned PDMS gasket as voids-free underfill material for implantable biomedical microsystems *Proc. IEEE Int. Microsystems, Packaging, Assembly and Circuits Technology Conf.* pp 81–4
[15] Khan S, Ordonez J S and Stieglitz T 2017 Dual-sided process with graded interfaces for adhering underfill and globtop

materials to microelectrode arrays *Proc. Int. IEEE EMBS Conf. on Neural Engineering* pp 247–50
[16] Ordonez J S, Boehler C, Schuettler M and Stieglitz T 2013 Silicone rubber and thin-film polyimide for hybrid neural interfaces—a MEMS-based adhesion promotion technique *Proc. IEEE EMBC Conf. on Neural Engineering* pp 872–5
[17] Benson R C, Farrar D and Miragliotta J A 2008 Polymer adhesives and encapsulants for microelectronic applications *John Hopkins APL Tech. Dig.* **28** 58–71
[18] Schuettler M *et al* 2008 Interconnection technologies for laser-patterned electrode arrays *Conf. Proc. IEEE. Engineering Medicine and Biology Society* pp 3212–5
[19] Kohler F, Ulloa M A, Ordonez J S, Stieglitz T and Schuettler M 2013 Reliability investigations and improvements of interconnection technologies for the wireless brain–machine interface-'BrainCon' *Proc. IEEE EMBC Conf. on Neural Engineering*
[20] Sutanto J, Anand S, Patel C and Muthuswamy J 2012 Novel first-level interconnect techniques for flip chip on MEMS devices *J. Microelectromech. Syst.* **21** 132–44
[21] Stieglitz T, Beutel H and Meyer J-U 2000 Microflex—a new assembling technique for interconnects *J. Intell. Mater. Syst. Struct.* **11** 417–25
[22] Meyer J-U, Stieglitz T, Scholz O, Haberer W and Beutel H 2001 High density interconnects and flexible hybrid assemblies for active biomedical implants *IEEE Trans. Adv. Packag.* **24** 366–74
[23] Jackson N and Muthuswamy J 2009 Flexible chip-scale package and interconnect for implantable MEMS movable microelectrodes for the brain *J. Microelectromech. Syst.* **18** 396–404
[24] Baek D-H *et al* 2011 Interconnection of multichannel polyimide electrodes using anisotropic conductive films (ACFs) for biomedical applications *IEEE Trans. Biomed. Eng.* **58** 1466–73
[25] Yang H S and Bakir M S 2012 Design, fabrication, and characterization of freestanding mechanically flexible interconnects using curved sacrificial layer *IEEE Trans. Compon. Packag. Manuf. Technol.* **2** 561–8
[26] Zhang C, Yang H S and Bakir M S 2014 Mechanically flexible interconnects (MFIs) with highly scalable pitch *J. Micromech. Microeng.* **24** 55024
[27] Shubin I *et al* 2009 Novel packaging with rematable spring interconnect chips for MCM *Proc. IEEE Electronic Components and Technology Conf.*
[28] Okereke R I and Sitaraman S K 2015 Mixed array of compliant interconnects to balance mechanical and electrical characteristics *J. Electron. Packag.* **137** 31006
[29] Kacker K, Sokol T, Yun W, Swaminathan M and Sitaraman S K 2007 A heterogeneous array of off-chip interconnects for optimum mechanical and electrical performance *J. Electron. Packag.* **129** 460
[30] Cheng B *et al* 2013 Microspring characterization and flip-chip assembly reliability *IEEE Trans. Compon. Packag. Manufact. Technol.* **3** 187–96
[31] Ordonez J S, Boehler C, Schuettler M and Stieglitz T 2012 Long-term adhesion studies of polyimide to inorganic and metallic layers *MRS Proc.* **1466** 7–13
[32] Grady M E, Geubelle P H and Sottos N R 2014 Interfacial adhesion of photodefinable polyimide films on passivated silicon *Thin Solid Films* **552** 116–23
[33] Chau K *et al* 2011 Dependence of the quality of adhesion between poly(dimethylsiloxane) and glass surfaces on the composition of the oxidizing plasma *Microfluid. Nanofluid.* **10** 907–17
[34] Schuettler M, Stiess S, King B V and Suaning G J 2005 Fabrication of implantable microelectrode arrays by laser cutting of silicone rubber and platinum foil *J. Neural Eng.* **2** S121–8
[35] Hassler C, Boretius T and Stieglitz T 2011 Polymers for neural implants *J. Polym. Sci.* B **49** 18–33
[36] Jaeger R D and Gleria M (ed) 2007 Inorganic polymers *Silicones in Industrial Applications* (New York: Nova Science Publishers) ch 2
[37] Balseal Engineering Inc 2017 Electrical contact solutions for medical active implantables www.balseal.com (Accessed: 21 October 2017)